NJC

Accepted Manuscript

This is an *Accepted Manuscript*, which has been through the Royal Society of Chemistry peer review process and has been accepted for publication.

Accepted Manuscripts are published online shortly after acceptance, before technical editing, formatting and proof reading. Using this free service, authors can make their results available to the community, in citable form, before we publish the edited article. We will replace this *Accepted Manuscript* with the edited and formatted *Advance Article* as soon as it is available.

You can find more information about *Accepted Manuscripts* in the Information for Authors.

Please note that technical editing may introduce minor changes to the text and/or graphics, which may alter content. The journal's standard Terms & Conditions and the Ethical guidelines still apply. In no event shall the Royal Society of Chemistry be held responsible for any errors or omissions in this *Accepted Manuscript* or any consequences arising from the use of any information it contains.

ROYAL SOCIETY OF CHEMISTRY

www.rsc.org/njc

New J.Chem

ARTICLE

Cajeput tree bark derived activated carbons for practical electrochemical detection of vanillin

Received 00th January 2015,
Accepted 00th January 2015

DOI: 10.1039/x0xx00000x

www.rsc.org/

Vediyappan Veeramani,[a] Rajesh Madhu,[a] Shen-Ming Chen,[*a] Pitchaimani Veerakumar,[b] Jhe-Jhen Syu,[a] and Shang-Bin Liu[*bc]

Cajeput tree bark derived activated carbons (TBACs) have been prepared and exploited for electrochemical detection of vanillin (VAN). The physicochemical properties of the TBACs graphitized at different temperatures were characterized by a variety of analytical and spectroscopic techniques, *viz*. X-ray diffraction, field emission-scanning/transmission electron microscopy (FE-SEM/TEM), N_2 adsorption/desorption isotherm measurements, and thermogravimetric analysis (TGA). Utilize as VAN sensors, the electrochemical activities of various TBAC- modified electrodes were assessed by cyclic voltammetry (CV) and linear sweep voltammetry (LSV). The superior electrocatalytic activity for oxidation of VAN observed is attributed to the high surface areas and desirable porosities possessed by TBAC. The VAN sensor exhibited a wide linear range (5–1150 μM), low detection limit (0.68 μM), and excellent sensitivity (0.32 μA mM^{-1} cm^{-2}), surpassing the existing carbon-based electrodes reported in the literature. The facile VAN sensor so realized is also advantaged by its simplicity, stability, reliability, durability, and low cost, rendering real sample analysis and practical industrial applications.

1. Introduction

Biomass-derived activated carbons (ACs) has been widely employed as electrode materials for applications in electrochemical biosensing, energy storage, removal of pollutants (*e.g.*, dyes and toxic metal ions) from aqueous solutions and so on.[1–6] This is mainly owing to the favorable properties, such as low cost, high surface area, and good electrical conductivity of the porous carbon-based electrode materials.[7–9] ACs prepared from renewable resources and biomass feedstocks such as water bamboo,[3] mango leaves,[6] coconut shell,[7] guava leaves,[10] water hyacinth,[11] pumpkin stem,[12] and an eggplant,[13] *etc*. have been reported and widely applied as cost-effective raw materials.

Melaleuca leucadendron (family: Myrtaceae), the Cajeput tree or *Melaleuca* tree, also commonly known as weeping paper barks, white paper barks, or punk tree,[14] are tall-growing trees (typically 20–30 m in height) highly cultivated in eastern Australia, Burma, New Guinea, the Solomon Islands, and the East Indies.[15] One of the most striking features of cajeput is its nearly pure-white papery bark, which may peel off in sheets. Parts of the plant are commonly prescribed traditionally as a remedy for diabetes mellitus. *Melaleuca* oil, whose primary constituent is cineol, is also used in medicine. Extracted solid terpineol, on the other hand, contains several aldehydes, such as valeric, butyric, and benzoic.[16] Its spongy tree bark is also commonly used as timber or for making shields, canoes,

[a] Department of Chemical Engineering and Biotechnology, National Taipei University of Technology, Taipei 10608, Taiwan. Tel: +886-2-27017147; Fax: +886-2-2702523.
E-mail: smchen78@ms15.hinet.net (S-M. Chen)
[b] Institute of Atomic and Molecular Sciences, Academia Sinica, Taipei 10617, Taiwan.
[c] Department of Chemistry, National Taiwan Normal University, Taipei 11677, Taiwan.

and roof. Paper bark tree is the outermost layer of stem and root of the woody plant. The cajeput trees are also enriched in lignocellulosic materials, however, it is necessary to break down the structure of the feedstock to obtain sugars from celluloses and hemicelluloses.[17] The aboundance of lignocelluloses in cajeput tree makes it a useful raw material for fabricating ACs. Herein, the tree bark has been chosen as the precursor to prepare the cajeput tree bark derived activated carbons (TBACs).

Vanillin (VAN) is considered as one of the most popular flavouring additive agents for beverages, cooking, and also being used as an aromatic additive for candles, incense, potpourri, fragrances, perfumes, and air fresheners.[18–20] VAN is also used as a starting material for the synthesis of drugs such as L-dopa, which is used for treating patients with Parkinson's disease. Basically, it is a phenolic aldehyde obtained from the extracts of vanilla bean. However, excessive ingestion of VAN may cause serious adverse effects such as allergy[21] and headaches,[22] and may also affect function of liver and kidney[23] and especially amelioration of depression, even at relatively low concentrations.[24] Several techniques have been reported for the quantitative determination of VAN, including gas chromatography (GC),[25] high-performance liquid chromatography (HPLC),[26] capillary electrophoresis (CE),[27] spectrophotometry,[28] and colorimetric analysis.[29] Nonetheless, the operation of these techniques, which invokes sophisticated instrumentations, is expensive, time-consuming, and also require a skilled operator to perform the experiment. Hence, the development of a facile technique for rapid, sensitive, and highly selective detection of VAN is a demanding task.[30–32]

Recently, the advancement in electrochemical sensors have attracted considerable attentions due to their advantages of rapid response, easy operation, high sensitivity, excellent selectivity, and capacities for real-time *in situ* detection. For example, Zheng *et al.*[33] reported the biosynthesis of Au–Ag alloy nanoparticles (NPs) by means of yeast cells and applied them to fabricate an electrochemical sensor for sensitive detection of VAN. Along the same line, an arginine functionalized graphene (Arg-G) nanocomposite was developed for the electrochemical sensing of VAN.[34] Nitrogen-doped graphene/carbon nanotubes (NGR-NCNT) nanocomposite prepared *via* the electrodeposition method has also been developed for simultaneous determination of caffeine and VAN.[35] Likewise, a hexagonal silver nanoparticles containing graphene (AgNPs-GN) nanocomposite modified glassy carbon electrode (GCE) has been applied as an electrochemical sensor for VAN detection.[36] Under optimized conditions, the calibration curve showed a linear range from 2 to 100 μM for detection of VAN with a detection limit of 3.32×10^{-7} M. Moreover, a new type of poly(allylamine hydrochloride) stabilized gold nanoparticles (AuNP-PAH) was also employed as sensors for the detection of VAN by using the square-wave voltammetry (SWV) technique, which exhibited a linear range from 0.90 to 15.0 μmol L^{-1} with a detection limit of 55 *n*mol L^{-1} and remarkable cycling stability.[37] These nanocomposite materials have been explored as promising materials in the development of electrochemical sensors for the detection of vanillin.[33–40]

In this study, we developed a novel and facile method for the synthesis of TBAC derived from biomass feedstock, namely cajeput tree bark, at different temperatures. The as-synthesized materials were characterized by various analytical techniques and have been successfully applied as a new electrochemical sensor for the detection of VAN, as illustrated in **scheme 1**. In particular, the TBAC-900 modified GCE exhibited an extraordinary electrocatalytic activity, sensitivity, selectivity, and desirable detection limit for VAN sample surpassing the other modified GCE.

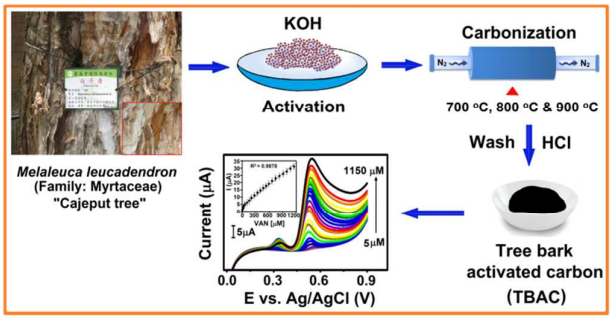

Scheme 1. Schematic illustration of the synthesis of TBACs derived from cajeput tree bark and their application as electrodes for VAN sensors.

2. Experimental section

2.1. Materials

Research grade Vanillin (VAN) and potassium hydroxide (KOH) was purchased (Sigma-Aldrich) without further purification. Cajeput tree barks (TB) were collected from the campus of National Taipei University of Technology in Taipei, Taiwan. A phosphate buffer solution (PBS) at pH 7.0 was prepared by using 0.05 M Na_2HPO_4 and NaH_2PO_4 solutions. The pH of the solution was adjusted with 0.5 M H_2SO_4 or 2.0 M NaOH. All other

chemicals used were analytical grade and all solutions were prepared by using ultrapure water (Millipore).

2.2. Characterization methods

The powder X-ray diffraction (XRD) studies were carried out by a Rigaku, MiniFlex II instrument. The surface morphology of various samples were probed by scanning electron microscopy (SEM; Hitachi S-3000 H) and field emission-transmission electron microscpy (FE-TEM; JEOL) operated at 300 kV. N_2 adsorption/desorption isotherm measurements at −196 ^oC were carried out on an Autosorb-1 system (Quantachrome). Prior to each measurement, the sample was out-gassed at 150 ^oC for 10 h under vacuum (10^2 Pa) to remove adsorbed water. The surface area of the sample was derived by the Brunauer-Emmett-Teller (BET) equation. The corresponding pore size was determined by means of non-linear density functional theory (NL-DFT) calculation. Cyclic voltammetry (CV) and linear sweep voltammetry (LSV) studies was accomplished by using a CHI 627 (CH instrument) electrochemical analyzer.

2.3. Synthesis of TBAC

The synthesis of biomass-derived AC was basically adopted from the procedure reported elsewhere.[10] In brief, the collected cajeput tree barks (TBs) were first cut into small pieces, followed by thorough washing with water, then dried in an oven at 100 ^oC . The dried TB strips were preheated at 200 ^oC for 6 h to remove the moisture, then, ground into a fine powder. The preheated TB powder were mixed with 10 % of KOH, followed by stirring at 60 ^oC under N_2 atmosphere for 24 h. Subsequently, *ca*. 2 g of the mixture was carbonized in a tube furnace at different temperatures (700, 800, and 900^oC) for 3 h in N_2 atmosphere with a heating rate of 5 ^oC min^{-1}. Finally the carbonized TBAC powder was washed with hot 1.0 M HCl and distilled water till reaching a pH of 7.0, then, dried at 100 ^oC overnight to obtain the final activated carbon materials, which are denoted hereafter as TBAC-T, where T represents the carbonization temperature in ^oC.

2.4. Preparation of TBAC-modified electrodes

To prepare the TBAC-modified GCE, *ca.* 5.0 mg of the as-prepared TBAC-T (T = 700, 800, and 900 ^oC) was dispersed in 1 mL ethanol, followed by sonication for 2 h. Prior to electrochemical studies, the surfaces of the modified GCE was carefully cleaned by 0.05 μm alumina powder, followed by sonication for several minutes with ethanol and deionized (DI) water. Subsequently, the TBAC-modified GCE was rinsed with DI water agaub to remove unbound TBAC material, followed by introducing an optimized concentration of test vanillin sample by drop casting method onto the TBAC-modified GCE at 30 ^oC in an air oven,. Finally, the TBAC-modified GCE was employed as the working electrode, while using Ag/AgCl (uder saturated KCl) as the reference electrode, and platinum wire as the counter electrode.

3. Results and discussion

3.1. Textural properties of TBAC materials

Figs. 1A-1C display the SEM images of various TBACs carbonized at different temperatures, denoted as TBAC-T, where T = 700, 800, or 900 ^oC. Among them, the TBAC-900 sample clearly shows the highly porous morphology with both micro- and meso-porosities. Upon increasing the carbonization temperatures, a notable increase in porosity of the ACs were evident.[41] The FE-TEM image of the TBAC-900 sample in **Fig. 1D** clearly reveals a honeycomb-like amorphous carbon structure. The high porosity possessed by the TBAC helps to reduce the diffusion path length of ions from the electrolyte, leading to enhancements in catalytic activity and sensitivity.

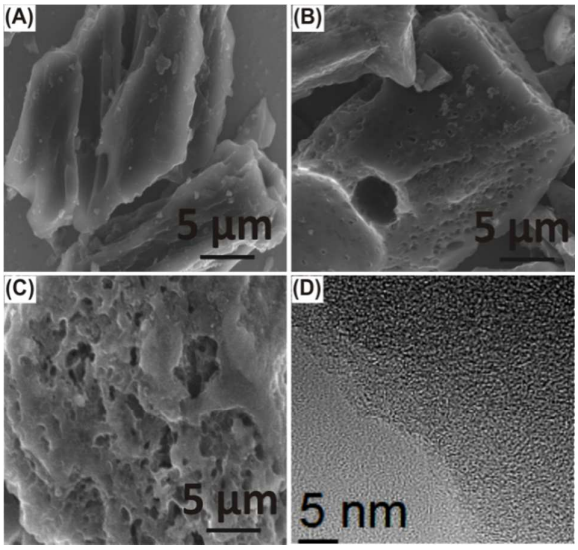

Fig. 1. SEM images of (A) TBAC-700, (B) TBAC-800, and (C) TBAC-900 samples. (D) high-resolution TEM image of the TBAC-900.

ARTICLE

Table 1. Physical properties of various as-synthesized samples.

Sample	Surface area ($m^2\ g^{-1}$)[a]		Pore volume ($cm^3\ g^{-1}$)[b]			D_p (nm)[e]
	S_{Total}	S_{Micro}[c]	V_{Total}	V_{Micro}[c]	V_{Meso}[d]	
TBAC-700	640	293	0.69	0.13	0.56	3.3
TBAC-800	935	425	0.74	0.19	0.55	3.7
TBAC-900	1234	536	0.75	0.23	0.52	4.0

[a] Brunauer–Emmet–Teller (BET) surface areas. [b] Total pore volume derived from the N_2 uptake at $P/P_0 = 0.99$. [c] Microporous surface area and pore volume obtained from *t*-plot analysis. [d] Mesoporous volume ($V_{Meso} = V_{total} - V_{Micro}$). [e] Pore size determined by the non-linear density functional theory (NL-DFT) calculation.

The XRD profile in **Fig. 2A** observed for the as synthesized TBAC-900 exhibits two broad diffractopm peaks at $2\theta = 21^o$ and 43^o, which may be attributed to the (002) and (100) planes, respectively. The results further confirm the existence of amorphous structure in the graphitized carbons. N_2 adsorption/desorption isotherms and pore size distribution curves of various carbon samples are shown in **Figs. 2B and 2C**, repectively. Accordingly, the corresponding textural parameters, including BET surface area, pore volume, and pore size, are depicted in **Table 1**. The N_2 adsorption/desorption curves observed for the TBACs reveal the typical Type-I isotherm based on the IUPAC classification, revealing the presence of both micro- and meso-porosities.[42,43] It is evident that the total surface area (S_{Total}) and total pore volume (V_{Total}) of the TBACs both increased with increasing carbonization temperature, mostly due to the increasing presence of microporosities.

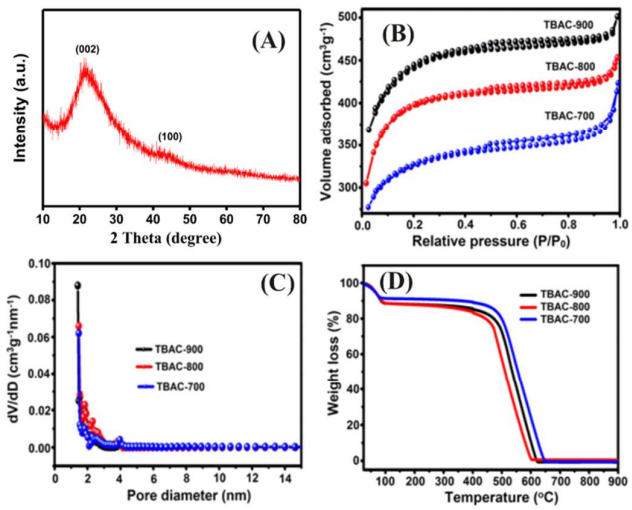

Fig 2. (A) XRD pattern of the TBAC-900 sample, and (B) N_2 adsorption/desorption isotherms, (C) pore size distribution, and (D) TGA curves of various as-synthesized TBACs.

The thermal stability of the TBAC framework was further studied by thermogravimetric analysis (TGA) and differential thermal analysis (DTA) under atmospheric air condition. Similar TGA curves were observed for various as-synthesized TGACs (in **Fig. 2D**), which revealed two weight-loss curves at ca. 100 and 450–650 ^oC, corresponding to the desorption of physisorbed water and pyrolysis of the carbon framework, respectively. These results show that these TBACs remain thermally stable at least up to 400 ^oC.

3.2. Electrochemical oxidation of vanillin

The electrocatalytic properties of the TBAC-modified GCE were investigated by CV technique, as shown in **Fig. 3A**. All CV curves were recorded in the presence of in the presence of 0.1 M PBS electrolyte (pH 7.0) together with 240 µM VAN at a constant scan rate of 50 mV s^{-1} The CV curves observed for the bare electrode (in absence of TBAC; **Fig. 3A**(a)) and the blank test (**Fig. 3A**(d)) revealed null oxidation signal, as expected. In contrast, CV profiles observed for the TBAC-modified GCE exhibited oxidation and reduction peaks in the presence of VAN. A well-defined oxidation peak (P1) appeared during the first segment and a reduction peak (P2) was obtained during the second segment, while another oxidation peak (P3) occurred during the third segment. Among the three samples examined, the TBAC-900 modified GCE showed the best electrocatalytic activity for VAN, revealing P1, P2, and P3 peaks at at +0.51, +0.26, and +0.31 V, respectively. Again, this may be ascribed due to the more abundant micro- and meso-porosities in the as-synthesized TBAC, which helps to absorb VAN more easily on the surfaces of the electrode. It is noteworthy that the intensity of the oxidation peak P1 tends to decrease slightly with increasing cycle segment, meanwhile, the intensities of the other two peaks (P2

and P3) increase slightly, then, remained stable afterword. Thus, it is indicative that peak P1 is irreversible and much more sensitive compared to the quasi-reversible redox couple peaks P2 and P3.[44] Moreover, the product of VAN appears to be irreversible.

3.3. Effect of scan rate and VAN concentration

The effect of scan rate on catalytic oxidation of VAN was studied by recording CV curves over the TBAC-900 modified GCE with varied scan rates, as shown in **Fig. 3B**. Notable increase in oxidation peak current with increasing scan rate was observed together with a slight positive shift in peak potential. Moreover, a linear correlation between the oxidation peak current and the square root of scan rate may be inferred by the linear regression equation: y = 0.5149x – 0.2295 with a coefficient of determination (R^2) of 0.9985. (see **Inset; Fig. 3B**). This indicates that the oxidation of VAN is a diffusion controlled process over the surfaces of the electrode. Accordingly, a reaction mechanism may be proposed, as illustrated in **Scheme 2**.

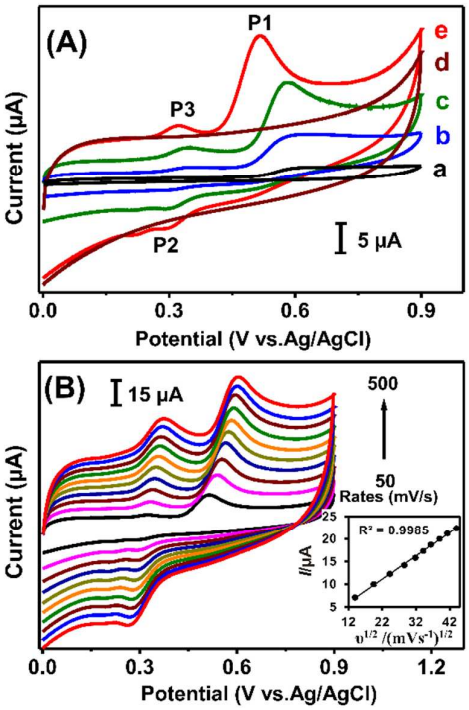

Fig 3. (A) CV curves of (a) bare electrode, and (b) TBAC-700, (c) TBAC-800, (e) TBAC-900 modified GCE in the presence of 0.1 M PBS (pH 7.0) electrolyte with 240 µM VAN recorded at a scan rate of 50 mV s^{-1}. Curve (d) shows the result of a blank measurement. (B) CV profiles recorded at different scan rates (50–500 mV s^{-1}). Inset: variations of peak oxidation current *vs* square root of scan rate.

Fig. 4A shows variations of CV curves with increasing concentration of added VAN (49–950 µM) over the TBAC-900 modified GCE. A linar correlation between the oxidation peak currents and VAN concentration was also observed (**Inset; Fig. 4A**).

3.4. Effect of electrolyte pH

The effect of pH of the electrolyte on electrocatalytic activity during oxidation of VAN was also investigated by CV measurements over

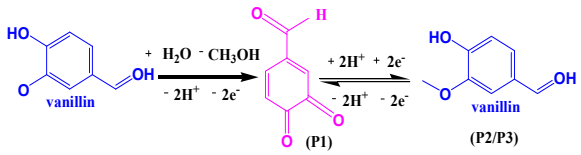

Scheme 2. The proposed reaction mechanism for the electrocatalytic reaction of VAN over the TBAC-modified GCE.

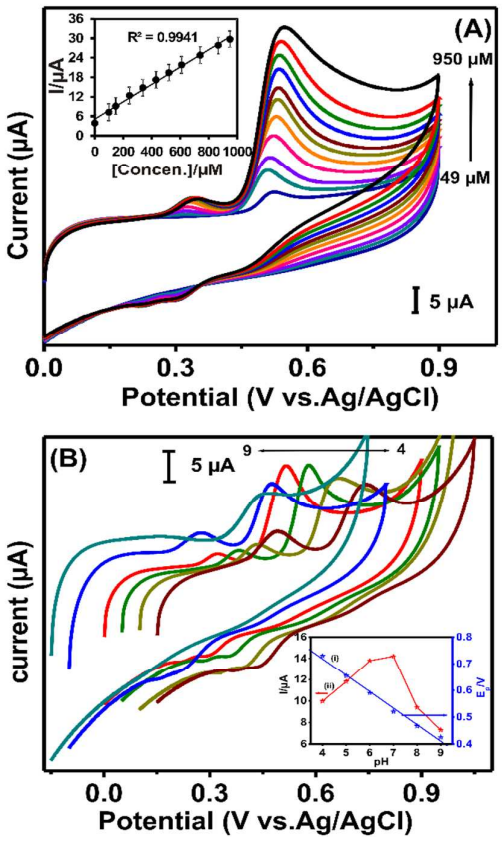

Fig. 4. CV curves of the TBAC-900 modified GCE with (A) varied concentrations of VAN (from 49 to 950 µM) in 0.1 M PBS (pH 7.0) solution recorded at a scan rate of 50 mV s^{-1} (Inset: plot of peak oxidation current *vs* VAN concentration), and (B) electrolyte pH (from 4.0 to 9.0). Inset: curve (i) plot of peak potential (E_p) vs pH; curve (ii) plot of peak oxidation current *vs* pH.

the TBAC-900 modified GCE by varing the pH of the PPS solution from 4.0 to 9.0 while in the presence of 240 µM VAN. The results are depicted in **Fig. 4B**, which revealed an optimized pH of *ca.* 7.0 (curve (ii); **Inset**), indicating that the reaction process was invoked by proton (H^+) mobility in the electrolyte solution. Moreover, notable shifting of the oxidation peak towards more negative potential was also found. As shown in **Fig. 4B**, a linear dependence between the peak potential (E_p) and electrolyte pH was observed (curve (ii); **Inset**) and may be fitted as: E_p (V) = –0.0616 (pH) + 0.9647 (R^2 = 0.9912). It is noted that a relative shift of 61.6 mV per pH unit, which is slightly higher than the theoretical value (57.6 mV/pH) may be inferred.[45] Accordingly, it is conclusive that the electron-transfer process during oxidation of VAN invoked an equal number of protons.

3.5. Accumulation studies

The influences of accumulation time and potential on electrooxidation of VAN were also examined. The results are shown in **Fig. 5**. Again, this was tested by recording CV curves over the BHAC-900 modified GCE under standard conditions (electrolyte: 0.1 M PBS, pH 7.0; VAN concentration 240 µM; scan rate of 50 mV s^{-1}). By varying the accumulation time while with a null accumulated potential of 0.0 V (**Fig. 5A**), a notable increase in the peak oxidation current was observed, reaching a maximum at 72 s, then declined gradually with prolonged accumulation time (**Fig. 5C**). Likewise, CV profiles were also recorded with varied accumulation potentials from –0.1 to +0.3 V (**Fig. 5B**), a maximum peak oxidation current was observed at an accumulated peak potential of 0.0 V (**Fig. 5D**). Thus, for experiments conducted hereafter, an accumulation potential of 0.0 V and an accumulation time of 72 s were used.

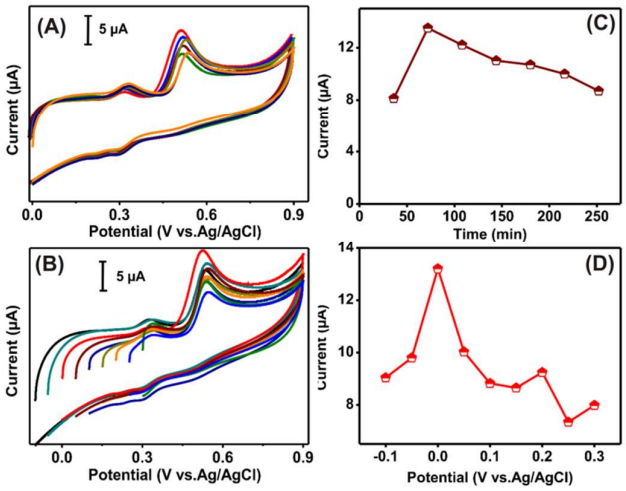

Fig. 5. Optimization of sensors: CV curves of the TBAC-900 modified GCE in 0.1 M PBS (pH 7.0) solution recorded with 240 µM VAN recorded at a scan rate of 50 mV s^{-1} with varied (A) accumulation time, and (B) accumulated potential, their corresponding variation with oxidation peak current are shown in (C) and (D), respectively (see text).

3.6. LSV studies

To further assess the sensitivity of the VAN sensor reported herein, LSV profiles were recorded under optimized experimental conditions (electrolyte pH 7.0; accumulated time 72 s; accumulated potential 0.0 V) with varied VAN concentrations. The results in **Fig. 6** clearly show that the peak oxidation current increases linearly with increasing concentration of VAN, as verify by the calibration plot (**Inset**; **Fig. 6**). It is noted that a linear regression equation may be fitted over a wide range of VAN concentration (5–1150 µM): I (µA) = 0.0253 (µM) + 3.4311 (R^2 = 0.9878). Accordingly, a sensitivity and a detection limit of 0.32 µA $µM^{-1}$ cm^{-2} and 0.684 µM, respectively, may be derived for the VAN sensor, whose performance suppassed most GCEs reported in the literature (**Table 2**).

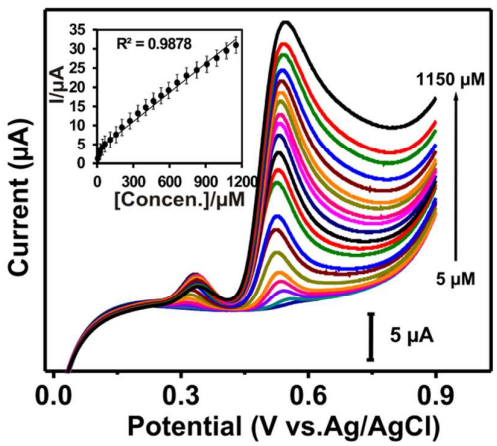

Fig. 6. LSV curves of TBAC-900 modified GCE with varied concentrations of VAN from 5–1150 μM in 0.1 M PBS (pH 7.0) solution recorded at a scan rate of 50 mV s^{-1}. Inset: plot of anodic oxidation peak current (I_{pa}) *vs* VAN concentration (μM).

3.7. Reproducibility, selectivity, and stability

The reproducibility, selectivity, and stability of the VAN sensor, which represent key parameter for practical applications, were also examined by the TBAC-900 modified GCE. To afford accessment of reproducibility, three independent TBAC-900 modified electrodes were tested in the presence of 240 μM VAN under standard conditions mentioned above. The measurements resulted in a relative standard deviation (RSD) of 2.5%, revealing a good reproducibility For selectivity studies, various potential interferences, such as NO^{3-}, K^{+}, Mg^{2+}, Fe^{3+}, Co^{2+}, Ni^{2+}, glucose, sucrose, and fructose, were added with an excessive relative concentration of 1,000 folds to the VAN. As a results, no observable change in the peak current of VAN was observed. In the co-presences of 50 folds excessive concentrations of ascorbic acid (AA), dopamine (DA), and uric acid (UA) with 240 μM VAN contained PBS solutions, only slight change in the observed peak oxidation current was found. These results reveal the promising selectivity of the VAN sensor reported herein. For stability test, a tested electrode was intentionally stored at room temperature for 25 days, more than 90% of its original peak oxidation current was retained, suggesting that the TBAC-modified electrode is suitable for practical catalytic applications.

3.8. Real sample analysis

The proposed VAN sensor is further tested using real food samples, namely a chocolate and a biscuit sample purchased from the local mart in Tapei, Taiwan. The chocolate and the biscuit samples were pretreated first by a thorough grounding in an agate mortar, leading to samples in form of fine powders. Then, typically *ca.* 1.0 g of the powder sample was dispersed in 5% ethanol and 95% buffer solution (pH = 7), followed by sonication treatment for 1 h and then filtered. For the test studies, pre-treated food sample was added consecutively onto 10 mL PBS solution, as shown in **Figs. 7(A)** and **7(B)** for the chocolate and the biscuit sample, respectively. The LSV results in **Fig. 7** clearly demonstrate that the TBAC-900 modified electrode is indeed highly suitable for real food sample analysis.

ARTICLE

Table 2. Electrochemical performances of various carbon-based electrode materials as sensor for detection of vanillin.

Material	Linear range (μM)	Detection limit (μM)	Technique	Reference
Ar[a]-Gr[b]/GCE[c]	2–70	1	DPV[i]	**34**
ENGR[d]-CNTs[e]/GCE	0.01–10	0.02	SWV[j]	**37**
Gr-PVP[f]/ABPE[g]	0.02–2, 0 2.0–40, and 40–100	0.01	DV[k]	**44**
AuPd-Gr/GCE	0.1–7 and 10–40	0.02	DPV	**46**
AgNPs[h]-Gr/GCE	2–100	0.33	SWV	**47**
Fe@Fe_3C-C/GCE	0.01–50	0.0026	DPV	**48**
MnO_2-Gr/GCE	0.03–8	0.0015	DPV	**49**
Gr/GCE	0.6–48	0. 05	DPV	**50**
GCE	50–300	0.16	SWV	**51**
TBAC-900/GCE	5–1150	0.68	LSV	**This work**

[a] Arginine; [b] Graphene; [c] Glassy carbon electrode. [d] Nitrogen-doped graphene; [e] carbon nanotubes; [f] Polyvinylpyrrolidone; [g] Acetylene black paste electrode; [h] Nanoparticles. [i] Differential pulse voltammetry; [j] Square wave voltammetry; [k] Derivative voltammetry.

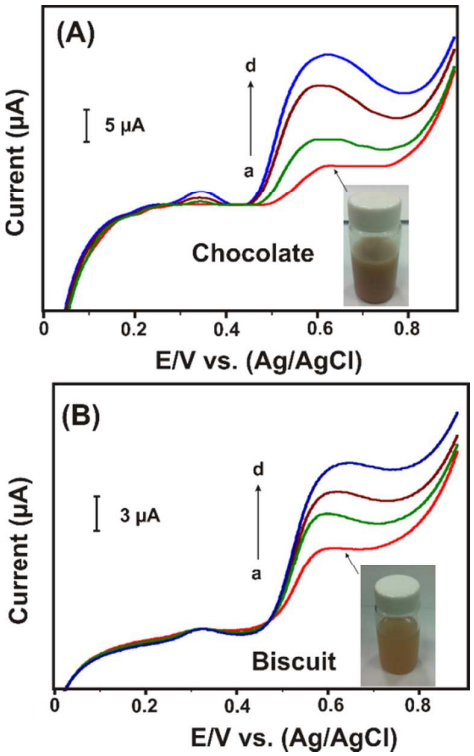

Fig. 7. LSV curves of TBAC-900 modified GCE in (A) chocolate and (B) biscuit samples. The the food samples containing VAN was added consecitively onto 0.1 M PBS (pH 7.0) buffer solution. All LSV curves were recorded at a scan rate of 50 mV s^{-1}.

4. Conclusions

We have demonstrated that the cajeput tree bark derived activated carbon (TBAC), which possess high surface areas and porosities desirable for sensitive detection of vanillin (VAN). When applied as VAN sensor, the TBAC-modified electrode, which exhibited low overpotential, wide linear range, suitable detection limit, and excellent sensitivity, reproducibility, selectivity, and stability even in presence of various interferences. The reported VAN sensor showed improved electrochemical performances compared to other carbon-based electrouterodes reported in the literature and showed perspective applications in real food sample analysis.

Acknowledgements

Financial supports for this work by the Ministry of Science and Technology (MOST), Taiwan (NSC101-2113-M-027-001-MY3 to SMC; NSC101-2113-M-001-020-MY3 to SBL) are gratefully acknowledged.

References

1. G.A. Ferrero, M. Sevilla and A.B. Fuertes, *Carbon* 2015, **88**, 239–251.
2. S.T. Senthilkumar, R.K. Selvan, J.S. Melo and C. Sanjeeviraja, *ACS Appl. Mater. Interfaces,* 2013, **5**, 10541−10550.
3. J. Li and Q. Wu, *New J. Chem.* 2015, **39**, 3859–3864.
4. Y. Chen and Y. Liu, *J. Mater. Chem. A*. 2014, **2**, 9193–9199.
5. K. Kadirvelu, M. Kavipriya, C. Karthika, M. Radhika, N. Vennilamani and S. Pattabhi, *Biores. Tech.* 2003, **87**, 129–132.

6. R. Madhu, K.V. Sankar, S.M. Chen and R.K. Selvan, *RSC Adv.,* 2014, **4**, 1225–1233.
7. Z. Hu and M.P. Srinivasan, Y. Ni, *Adv. Mater.* 2000, **12**, 62–65.
8. J. Wang and S. Kaskel, *J. Mater. Chem.,* 2012, **22**, 23710–23725.
9. M. Sevilla and R. Mokaya, *Energy Environ. Sci.,* 2014, **7**, 1250–128.
10. R. Madhu, V. Veeramani, S.M. Chen, P. Veerakumar and S.B. Liu, *Chem. Eur. J.* 2015, **21**, 8200–8206.
11. X. Liu, Y. Zhou, W. Zhou, L. Li, S. Huang and S. Chen, *Nanoscale* 2015, **7**, 6136–6142.
12. R. Madhu, V. Veeramani, S.M. Chen, J. Palanisamy and A.T.E. Vilian, *RSC Adv.,* 2014, **4**, 63917–63921.
13. Z. Li, W. Lv, C. Zhang, B. Li, F. Kang and Q.H. Yang, *Carbon* 2015, **92**, 11–14.
14. N. Ahmed, S.P. Santoso, P.L. Tran-Nguyen, L.H. Huynh, S. Ismadji and Y.H. Ju, *Bioresource Technol.,* 2013, **139**, 410–414.
15. K.A. Hammer, C.F. Carson, T.V. Riley and J.B. Nielsen, *Food Chem. Toxicol.* 2006, **44**, 616–625.
16. R.C. Padalia, R.S. Verma, A. Chauhan and C.S. Chanotiya, *Indus. Crops. Products,* 2015, **69**, 224–227.
17. I.N. Ahmed, P.L.T. Nguyen, L.H. Huynh, S. Ismadji and Y.H. Ju, *Bioresour. Technol.,* 2013, **136**, 213–221.
18. E. Anklam and S. Gaglione, A. Muller, *Food Chem.,* 1997, **60**, 43–51.
19. N.J. Walton, M.J. Mayer and A. Narbad, *Phytochemistry*, 2003, **63**, 505–515.
20. L. Shang, F. Zhao and B. Zeng, *Food Chem.,* 2014, **151**, 53–57.
21. H. van Assendelft. *British Medical J.* 1987, **294**, 576– 577
22. M. Saint-Denis, M.W. Coughtrie, J.C. Guilland, B. Verges, M. Lemesle and M. Giroud, *Presse Médicale* 1996, **25**, 2043.
23. Y. Ni, G. Zhang and S. Kokot, *Food Chem.,* 2005, **89**, 465–473.
24. J. Xu, H. Xu, Y. Liu, H. He and G. Li, *Psychiatry Res.,* 2015, **225**, 509–514.
25. T. Sostaric, M.C. Boyce and E.E. Spickett, *J. Agric. Food Chem.*, 2000, **48**, 5802–5807.
26. G. Lamprect, F. Pichlmayer and E.R. Schmid, *J. Agric. Food Chem.,* 1994, 42, 1722–1727.
27. M.C. Boyce, P.R. Haddad and T. Sostaric, *Anal. Chim. Acta,* 2003, **485**, 179–186.
28. Y. Ni, G. Zhang and S. Kokot, *Food Chem.,* 2005, **89**, 465–473.
29. H. Peng, S. Wang, Z. Zhang, H. Xiong, J. Li, L. Chen and Y. Li, *J. Agric. Food Chem.,* 2012, **60**, 1921−1928.
30. M.A. Xinying, *Int. J. Electrochem. Sci.,* 2014, **9**, 3181−3189.
31. G.M. Durán, A.M. Contento and Á. Ríos, *Talanta* 2015, **131**, 286–291
32. F. Bettazzi, I. Palchetti, S. Sisalli and M. Mascini, *Anal. Chimi. Acta.,* 2006, **555**, 134–138.
33. D. Zheng, C. Hua, T. Gan, X. Dang and S. Hu, *Sens.Actuators B.* 2010, **148**, 247–252.
34. Y. Zhao, Y. Du, D. Lu, L. Wang, D. Ma, T. Ju and M. Wu, *Anal. Methods,* 2014, **6**, 1753–1758.
35. J.Y. Peng, C.T. Hou and X.Y. Hu *Inter. J. Electrochem. Sci.,* 2012, **7**, 1722–1733.
36. L. Huang, K. Houb, X. Jia, H. Pan and M. Du, *Mater. Sci. Eng. C*, 2014, **38**, 39–45.
37. S. Luo and Y. Liu, *Int. J. Electrochem. Sci.*, 2012, **7**, 6396–6405.
38. L. Jiang, Y. Ding, F. Jiang, L. Li and F. Mo, *Anal. Chim. Acta*, 2014, **833**, 22–28.
39. T.R. Silva, D. Brondani, E. Zapp and I.C. Vieira, *Electroanalysis* 2015, **27**, 465–472.
40. J. Sun, T. Gan, K. Wang, Z. Shi, J. Li and L. Wang, *Anal. Methods,* 2014, **6**, 5639–5646.
41. L. Qie, W. Chen, H. Xu, X. Xiong, Y. Jiang, F. Zou, X. Hu, Y. Xin, Z. Zhang and Y. Huang, *Energy Environ. Sci.,* 2013, **6**, 2497–.
42. Z. Hu, M.P. Srinivasan and Y. Ni, *Adv. Mater.*. 2000, **12**, 62–65.
43. G. Xu, J. Han, B. Ding, P. Nie, J. Pan, H. Dou, H. Li and X. Zhang. *Green Chem.***,** 2015, **17,** 1668–1674.
44. P. Deng, Z. Xu, R. Zeng and C. Ding. *Food Chem.,* 2015, **180**, 156–163.
45. J. Bard and L.R. Faulkner. *Electrochemical methods: Fundamentals applications*, 2nd Ed. New York: Wiley, 2001.
46. L.Shang, F. Zhao, B. Zeng. *Food Chem.,* 2014, **151**, 53–57.
47. L. Huang, K. Hou, X. Jia, H. Pan, M. Du. *Mater. Sci. Eng. C,* 2014, **38**, 39–45.
48. J. Sun, T. Gan, K. Wang, Z. Shi, J. Li and L. Wang. *Anal. Methods,* 2014, **6**, 5639-5646.
49. T. Gan, Z. Shi, Y. Deng, J. Sun, H. Wang. *Electrochimica Acta,* 2014, **147**, 157–166.
50. J. Peng, C. Hou, X. Hu, *Int. J. Electrochem. Sci.,* 2012, **7**, 1724 – 1733.
51. J.L. Hardcastle, C.J. Paterson, R.G. Compton, *Electroanalysis* 2001, **13**, 899-905.

Graphical Abstarct

Title: Cajeput tree bark derived activated carbons for practical electrochemical detection of vanillin

Vediyappan Veeramani,[a] Rajesh Madhu,[a] Shen-Ming Chen,[*a] Pitchaimani Veerakumar,[b] Jhe-Jhen Syu,[a] and Shang-Bin Liu[*bc]

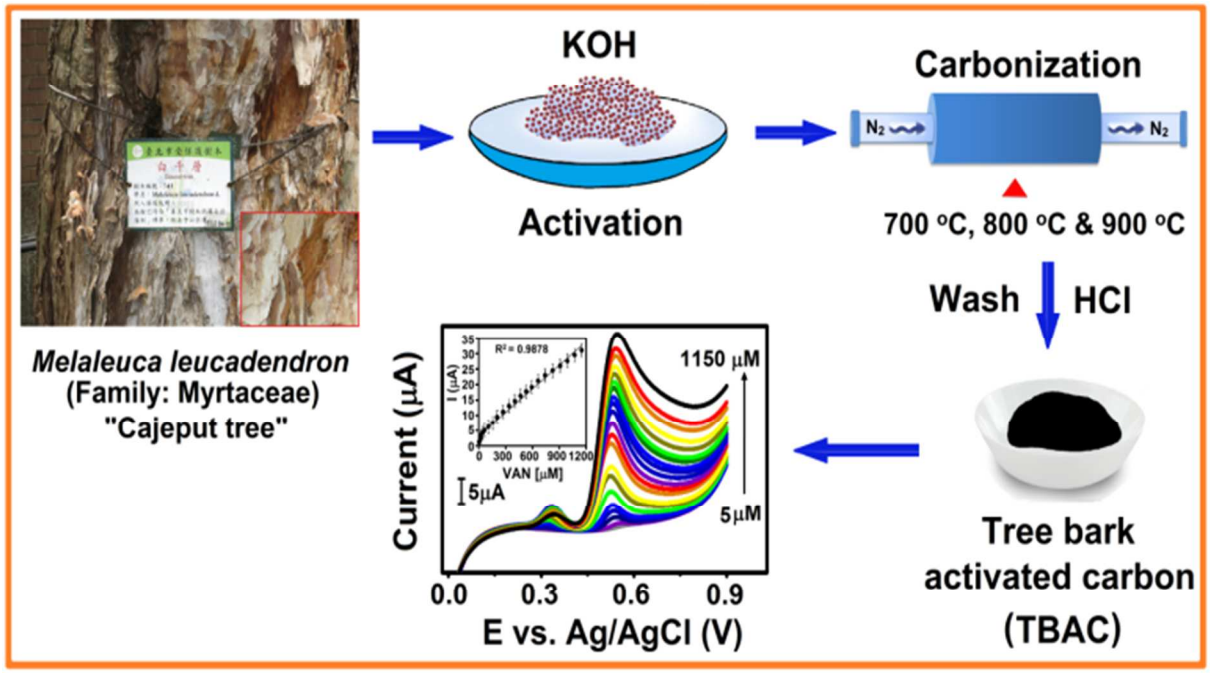

A facile synthesis stratergy for fabrication of cajeput tree bark derived functional porous carbons and their applications as vanillin sensor is reported.